Establishment and evaluation of a co-effect structure with thermal concentration–rotation function in transient regime*

Yi-yi Li(李依依) and Hao-chun Zhang(张昊春)†

School of Energy Science and Engineering, Harbin Institute of Technology, Harbin 150001, *China*

(Received 18 March 2020; revised manuscript received 17 April 2020; accepted manuscript online 19 May 2020)

The advanced heat flux manipulating structures inspired by TO-based spatial mapping have aroused wide interests owing to huge potential in high-efficient thermal energy utilization. However, most researches are limited to the realization of single function in one specific structure and appropriate evaluation of the energy transfer process is relatively lacking. In this work, based on time-dependent two-dimensional heat conduction equation, a co-effect structure capable of accomplishing concentration and rotation functions simultaneously is established and validated by finite element simulations compared with the conventional single concentrator and singe rotator. In addition, from the perspective of thermodynamics, the transformed local entropy production rate and total entropy production are theoretically derived and applied to evaluate the quality of energy transfer processes. The proposed co-effect structure can help to explore other potential mass/flux manipulating devices and the evaluation method is valuable for the further manufacturing as well as optimization of these devices in engineering applications.

Keywords: transformation thermodynamics, thermal concentration–rotation transformed entropy production, transient regime

PACS: 44.10.+i, 44.05.+e **DOI:** 10.1088/1674-1056/ab9437

1. Introduction

Effective energy management is much necessary and valuable for both science and industry, the significant transformation optics (TO) theory raised in 2006[1] is undoubtedly an essential tool to achieve this goal. The key of this theory is to connect the original space and the virtual space through curvilinear coordinate transformation method under the control of form-invariant equation, the consequent distribution of properties are fabulous and impossible to find in conventional materials, which can be utilized to build functional mass/flux manipulating devices. After the theoretical design[1] and experimental demonstration[2] of the first electromagnetic metamaterial cloak which is able to hide an arbitrary object without disturbing the external field, this kind of inconceivable structure as well as other derivatives including concentrators, rotators, camouflages, lenses, *etc*., have aroused wide concern in the fields of electromagnetics,[3–5] optics,[6–8] acoustics,[9–11] and elastodynamics.[12,13] Since the form-invariant characteristic of heat conduction equation has been verified transformation thermodynamics theory an analogue of TO theory, has been put forward to innovatively manipulating heat flux using thermal metamaterial.[14] Spherical and spheroidal thermal cloaks as the most typical heat flow control devices were designed and apparent negative thermal conductivity (ANTC) were observed.[15] Thermal cloak under anisotropic background was studied through mathematical treatments.[16] Using effective medium theory and multilayered composite structure, thermal cloak was experimentally verified with regular materials[17] and different types of cloaking structures were realized based on them.[18,19] Besides thermal concentrator was also established with transformation thermodynamics method[15] and a fan-shaped composite counterpart apparently worked.[20] To improve the flexibility and universality, a new design method was proposed which is of great value for engineering fabrication.[21] Concentrating effect was also achieved under thermal convection conditions.[22] What is more, theoretical accounts as well as simulated verifications of thermal rotator were implemented.[20] Research on other peculiar heat phenomena including illusion,[23,24] thermal printing,[25] and diodes[26] have made much progress either.

For most of researches, heat flux manipulation structures usually performed single function. However, the coexistence of two or more effects in certain device possesses more engineering value since it can better satisfy the potential different needs in actual use.[27] What is more, an appropriate assessment index is required for each physically meaningful energy transfer process and thermodynamic criterions represented with local entropy production rate and total entropy production are suitable to judge the quality of different heat transfer processes.[28–31] In this paper, based on time-dependent two-dimensional heat conduction equation, we propose a co-effect structure to achieve concentration and rotation effects simultaneously by implementing coordinate transformation in different directions. Through finite-element simulation, the thermal response and fundamental mechanism of this

*Project supported by the National Natural Science Foundation of China (Grant Nos. 51776050 and 51536001).

†Corresponding author. E-mail: hczhang@hit.edu.cn

dual-function structure are theoretically analyzed and compared with the traditional concentrator and rotator with single effect. Furthermore, considering the thermodynamic properties of the system, the local entropy production rate and the total entropy production based on transformed coordinates are derived and used to investigate the quality and irreversible energy loss in different processes.

2. Theoretical description

Diagram in Fig. 1 shows the spatial transformation principle for the coexistence of concentrating and rotating effects. The annulus with interval $R_2 < r < R_3$ was stretched toward the origin along the radial direction, forming a smaller core region with radius R_1. Meanwhile, this core region is rotated by an angle of θ_0 as the red arrow indicates. This change gradually recovers the new area $R_1 < r < R_3$ and eventually vanishes on the outside boundary with the blue arrow keeps still. As a result, the desired system in the transformed coordinates can be mapped onto the original coordinates.

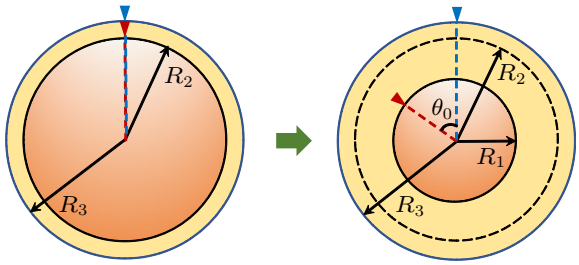

Fig. 1. Diagram of spatial transformation process.

Referring to transformation thermodynamics,[15] the transformed time-dependent two-dimensional heat conduction equation neglecting inner source can be written as

$$\rho' c' \frac{\partial T}{\partial t} = \nabla \cdot (\kappa' \nabla T), \tag{1}$$

where t is time, T is the distribution of temperature field when $t > 0$, ρ' represents transformed density, and c' represents transformed specific thermal capacity. κ' is transformed thermal conductivity which cannot be extracted in front of the differential operator since spatial derivations are taken to guarantee continuity of heat flux. Considering the coordinate mapping from virtual space to original space, that is, from $\{x', y'\}$ to $\{x, y\}$, this connection can be established by Jacobin matrix

$$J = \frac{\partial(x', y')}{\partial(x, y)} = J_{x'r'} J_{r'r} J_{rx} = \frac{\partial(x', y')}{\partial(r', \theta')} \frac{\partial(r', \theta')}{\partial(r, \theta)} \frac{\partial(r, \theta)}{\partial(x, y)}, \tag{2}$$

where $J_{x'r'}$, $J_{r'r}$, and J_{rx} respectively denote the compound Jacobin matrix of co-ordinates. Then we can obtain the expression of transformed thermal conductivity κ' with the Jacobin matrix involved as

$$\kappa' = \frac{J \kappa_0 J'}{\det(J)}, \tag{3}$$

where κ_0 denotes the thermal conductivity in the original space. Corresponding to the expected spatial expansion, compression, and rotation in Fig. 1, the geometric transformation in different directions can be expressed as

$$\begin{cases} r' = \dfrac{R_1}{R_2} r, & (0 < r \le R_1), \\ r' = \dfrac{R_3 - R_1}{R_3 - R_2} r + \dfrac{R_1 - R_2}{R_3 - R_2} R_3, & (R_1 < r \le R_3), \\ r' = r, & (r > R_3), \end{cases} \tag{4}$$

$$\begin{cases} \theta' = \theta + \theta_0, & (0 < r \le R_1), \\ \theta' = \theta + \theta_0 \dfrac{R_3 - r}{R_3 - R_1}, & (R_1 < r \le R_3), \\ \theta' = \theta, & (r > R_3). \end{cases} \tag{5}$$

Thus, the transformed region can go through radial stretching and gradual azimuthal rotation from inner to outer at the same time. From Eqs. (2)–(5), we can deduce expressions of the Jacobin matrix as

$$J = R(\theta') \operatorname{diag}(1, r') \begin{bmatrix} \dfrac{R_1}{R_2} & 0 \\ 0 & 1 \end{bmatrix} \operatorname{diag}(1, 1/r) R(\theta)^{\mathrm{T}}, \quad (0 < r \le R_1), \tag{6}$$

$$J = R(\theta') \operatorname{diag}(1, r') \begin{bmatrix} \dfrac{R_3 - R_1}{R_3 - R_2} & 0 \\ \dfrac{-\theta_0}{R_3 - R_1} & 1 \end{bmatrix} \operatorname{diag}(1, 1/r) R(\theta)^{\mathrm{T}}, \quad (R_1 < r \le R_3), \tag{7}$$

where $R(\theta')$ and $R(\theta)$ are the rotation (unimodular) matrices between Cartesian coordinate and cylindrical coordinate. Note that $R(\theta')^{\mathrm{T}} = R(\theta')^{-1}$, the transformed thermal conductivity in different domains can be obtained finally

$$\kappa' = R(\theta') \begin{bmatrix} \kappa'_{xx} & \kappa'_{xy} \\ \kappa'_{yx} & \kappa'_{yy} \end{bmatrix} R(\theta')^{-1} = R(\theta') \operatorname{diag}(1, 1) R(\theta')^{-1} \kappa_0, \quad (0 < r \le R_1), \tag{8}$$

$$\kappa' = R(\theta') \begin{bmatrix} \kappa'_{xx} & \kappa'_{xy} \\ \kappa'_{yx} & \kappa'_{yy} \end{bmatrix} R(\theta')^{-1} = R(\theta') \begin{bmatrix} \dfrac{T}{r'(R_2 - R_3)} & \dfrac{\theta_0 T}{(R_1 - R_3)^2} \\ \dfrac{\theta_0 T}{(R_1 - R_3)^2} & \dfrac{r' \theta_0^2 (R_3 - R_2) T}{(R_1 - R_3)^4} + \dfrac{r'(R_3 - R_2)}{T} \end{bmatrix} \times R(\theta')^{-1} \kappa_0, \quad (R_1 < r \le R_3), \tag{9}$$

where $T = r'(R_3 - R_2) - R_3(R_1 - R_2)$. From these derivations we can easily find that more anisotropic thermal conductivity appears in the region of $R_1 < r < R_3$. By substituting Eq. (8) and Eq. (9) into Eq. (1), we can detail the transformed heat conduction equation as

$$\rho' c' \frac{\partial T}{\partial t} = \frac{\partial}{\partial x'} \left(R(\theta') \begin{bmatrix} \kappa'_{xx} & \kappa'_{xy} \end{bmatrix} R(\theta')^{-1} \frac{\partial T}{\partial x'} \right) + \frac{\partial}{\partial y'} \left(R(\theta') \begin{bmatrix} \kappa'_{yx} & \kappa'_{yy} \end{bmatrix} R(\theta')^{-1} \frac{\partial T}{\partial y'} \right), \tag{10}$$

where the transformed product of density by specific thermal capacity can be calculated by $\rho' c' = \det(J)\rho c$. In order to better investigate the quality of the energy transfer process in view of thermodynamics, local entropy production rate[28] for two-dimensional domain is introduced. For isotropic and homogenous medium without spatial change, there is

$$\dot{S}_g'' = \frac{\kappa}{T^2}\left[\left(\frac{\partial T}{\partial x}\right)^2 + \left(\frac{\partial T}{\partial y}\right)^2\right]. \tag{11}$$

While for the transformed area, the expression needs to be modified as

$$\begin{aligned}\dot{S}_g'' &= \frac{\partial}{\partial x'}\left(\frac{q_x'}{T}\right) + \frac{\partial}{\partial y'}\left(\frac{q_y'}{T}\right)\\ &= \frac{\partial}{\partial x'}\left(\frac{-1}{T}R(\theta')\begin{bmatrix}\kappa_{xx}' & \kappa_{xy}'\end{bmatrix}R(\theta')^{-1}\frac{\partial T}{\partial x'}\right)\\ &\quad + \frac{\partial}{\partial y'}\left(\frac{-1}{T}R(\theta')\begin{bmatrix}\kappa_{yx}' & \kappa_{yy}'\end{bmatrix}R(\theta')^{-1}\frac{\partial T}{\partial y'}\right)\\ &= \frac{-1}{T^2}\begin{bmatrix}\left(\frac{\partial T}{\partial x'}\right)^2 & \left(\frac{\partial T}{\partial y'}\right)^2\end{bmatrix}\cdot R(\theta')\cdot\begin{bmatrix}\kappa_{xx}' & \kappa_{yx}'\\ \kappa_{xy}' & \kappa_{yy}'\end{bmatrix}\cdot R(\theta')^{-1}\\ &= \begin{bmatrix}\dot{S}_{gx}'' & \dot{S}_{gy}''\end{bmatrix}. \end{aligned}\tag{12}$$

Due to the fact that the apparent anisotropy and heterogeneity result from spatial changes in different directions, the transformed local entropy production rate is a matrix of two components rather than a single value. Then the expression of the transformed total entropy production can be written as

$$\dot{S}_{\mathrm{g}} = \sum \iint_A \dot{S}_{\mathrm{g}}'' \mathrm{d}A, \tag{13}$$

where A denotes area of different integration parts which can be divided randomly to serve the calculation. This additive feature allows the transformed total entropy production to act as a characteristic parameter of the whole system. Next, aiming at the proposed co-effect as well as comparison with the single concentration and single rotation function, the heat conduction equation inserted with anisotropic heterogeneous thermal conductivity is numerically solved by finite element method using commercial package COMSOL MULTIPHYSICS.

3. Results and discussions

From temperature profiles in Fig. 2, we can clearly observe the functional differences among three structures in each transient state. For the background area outside the function region under all conditions, the heat flux uniformly propagates from the high temperature end to the low temperature end and keeps parallel to the x axis all the time, implying that the external environment is not affected by the spatial transformation in the central part. Once the heat flux enters the transform-based annuls region, the single concentrator in Fig. 2(a) drives the heat flux toward the origin in the radial direction and the temperature gradient in the core region is enhanced to be 575 K/cm, which is 1.53 times the applied gradient. Figure 2(b) shows that the single rotator gradually rotated the heat flux in annuls region and finally the heat flux is converted by the pre-specified angel $\theta = \pi/3$ in core circle region. However, for the proposed co-effect structure in Fig. 2(c), the heat flux is not only concentrated in the core region, resulting in a higher temperature gradient, but also regulates counter cloak wise by a weaker rotation effect compared to the single rotator. This is better displayed in pictures at $t = 0.3$ s with reduced deflection of arrows, but still an apparent rotation effect can be observed compared to the single concentrator.

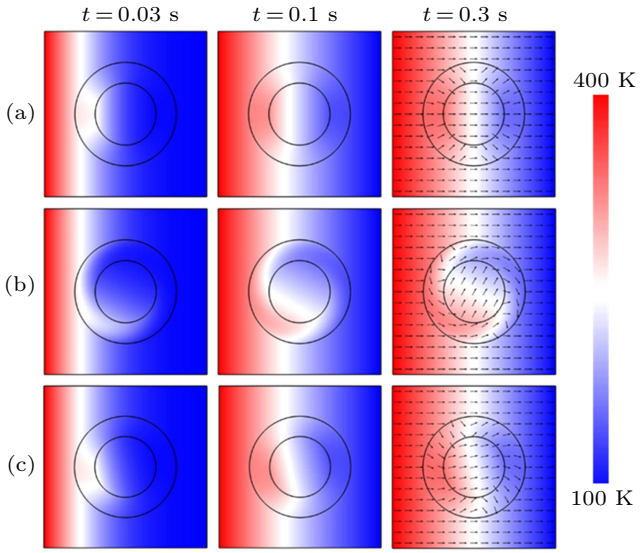

Fig. 2. Transient temperature profiles of three structures at different times: (a) single concentrator, (b) single rotator, (c) co-effect structure, the black arrows represent heat flux. The dimension of the whole simulation domain is 0.8 cm × 0.8 cm, both upper and lower boundaries are thermally isolated, left and right boundaries are respectively fixed at temperature $T = 400$ K and $T = 100$ K, leading to an applied temperature gradient of 375 K/cm. The medium of background area outside the function region is set with $\kappa_0 = 0.16$ W/(m·K) and $\rho c = 1.358 \times 10^{-3}$ MJ/(m^3·K) and thermal conductivity of the transformed domain are arranged as theoretical work. The geometric parameters of annuls region are set as $R_1 = 0.15$ cm, $R_2 = 0.23$ cm, and $R_3 = 0.25$ cm.

In order to make quantitative description, a measured line $x = -0.05$ cm is chosen and figure 3(b) shows the temperature variations of the above structures on this measured line. The measured line is chosen following the direction of the isothermal line that is perpendicular to x axis, so the effects of different embedded structures on the temperature field can be reflected by the shape of curves. In addition, the spatial deformation degree varied with locations in each structure, changes in temperature on vertical measured line passing though the origin is relatively small and insufficient to intuitively perform the characteristics of devices, especially for the single thermal concentrator. Thus, $x = -0.05$ cm is chosen as the measured line to obtain more clear results for subsequent analysis and discussion. Compared with the single concentrator, the co-effect structure apparently rotates the temperature field in the

core region and the curves varies with the pre-designed rotation angel θ_0. At a fixed θ_0, the changing magnitude of temperature curves in both annuls and core regions of the co-effect structure is much smaller than that of the single rotator, leading to reduced heat dissipation and energy randomness. As approaching the outer boundary of the annuls, temperature drops or increases rapidly, finally temperature curves of background area in all schemes keep parallel to the y direction of the simulation domain and overlapped with each other, representing an unaffected external field.

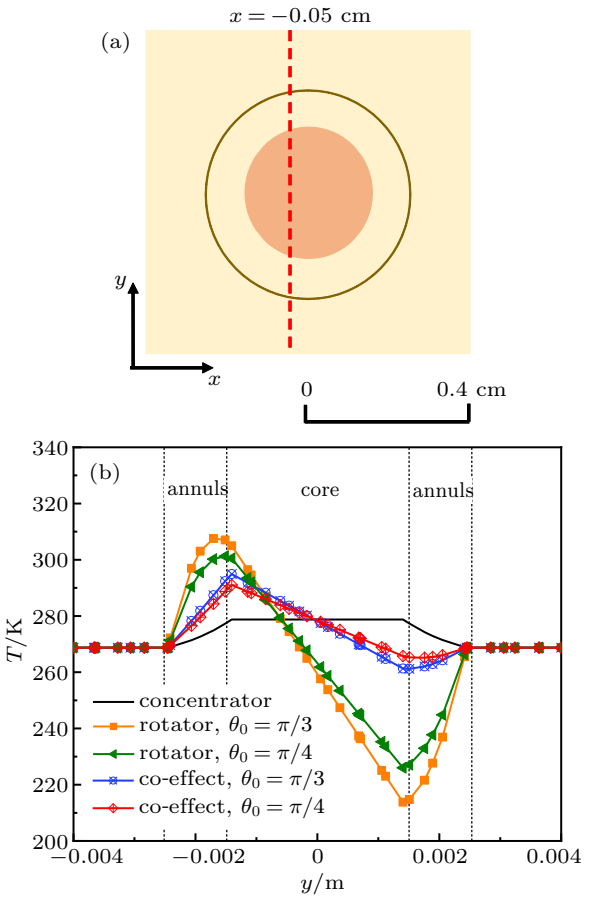

Fig. 3. (a) Diagram of measured line, (b) temperature distribution on the measured line along y direction of three structures.

According to our theoretical work, different components of the transformed local entropy production rate at $t = 0.3$ s of three structures are pictured individually in Fig. 4. In the background area, analogue to a uniform temperature field and undisturbed heat flux, both components respectively show the same characteristics in different structures where $\dot{S}''_{gx}$ increases from left to right because temperature varies conversely and $\dot{S}''_{gy}$ keeps constant since the temperature gradient along y axis is zero, indicating that embedded distorted spaces have no influence on the surrounding background. In the annuls part, $\dot{S}''_{gx}$ of the single concentrator mainly distributes on diagonal region especially near the low temperature end, implying the radial enter or leave of heat flux caused most heat dissipation and energy loss. Chaos of thermal energy and disturbance of thermal field are much more severe in the single rotator and most $\dot{S}''_{gx}$ appeared at the pre-designed rotation angle where huge temperature difference exists. The distribution of $\dot{S}''_{gx}$ in co-effect structure is similar to that of the single concentrator except the position azimuthally varied corresponding to but smaller than the pre-designed rotation angle, and the overall value increases but still far lower than single rotator. Besides, $\dot{S}''_{gx}$ in the core region performs uniformly in all structures, the numerical value of the single rotator is slightly lower because of less spatial transformation. For $\dot{S}''_{gy}$ in three structures, the configuration is basically identical with $\dot{S}''_{gx}$, numerical differences in local positions are the result of different anisotropy thermal conductivity and temperature gradients. Judging from temperature profiles and distributions of the transformed local entropy production rate in different structures, it is reasonable to speculate that the concentration of heat flux can noticeably reduce the disorder of thermal energy caused by the rotation effect, leading to a more even thermal field and less thermal energy loss.

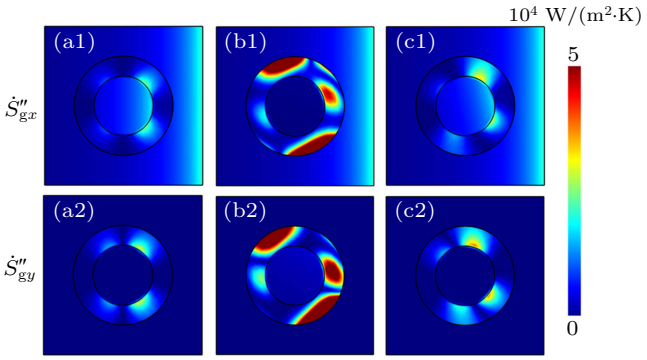

Fig. 4. Profiles of components of the transformed local entropy production rate at $t = 0.3$ s in three structures: (a1) and (a2) single concentrator; (b1) and (b2) single rotator; (c1) and (c2) co-effect structure.

As a key factor to manipulate heat flux, variations of each constitute of anisotropic thermal conductivity in transformed domain from inner boundary to outer boundary with different pre-designed parameter are displayed in Fig. 5 to explore the potential mechanism behind the above thermal phenomena. Based on our theoretical derivations and previous work,[27] the three structures own the same deformation in the core region, for simplicity we only show the constitutes of anisotropic thermal conductivity in annuls part. In Fig. 5(a), κ'_{xx} is independent of the pre-designed rotation angle in all structures and equal to 1 at every position in the single rotator. For the single concentrator and the co-effect structure, κ'_{xx} possesses the same changing regulation that decreases in exponential form with the increase of the radial distance. The diagonal terms κ'_{xy} (κ'_{yx}) of different structures in Fig. 5(b) are distinct from each other, which remains zero all the time in the single concentrator but linearly decreases as the radial distance increases in other two structures with more obvious gradient in the single rotator. Large pre-designed angle contributes to enhanced

component of thermal conductivity with a minus sign, and the co-effect structure always shows a larger absolute value than the single rotator at a fixed angle although this difference gradually reduces and vanishes at the outer boundary of the annuls. In Fig. 5(c), κ'_{yy} is directly proportional to the increasing radial change. The pre-design rotation angle lifts not only the values but also the changing gradient of κ'_{yy}, both of which are the highest in the single rotator. Under the same conditions, κ'_{yy} of the co-effect structure is much lower than the single rotator while higher than the single concentrator.

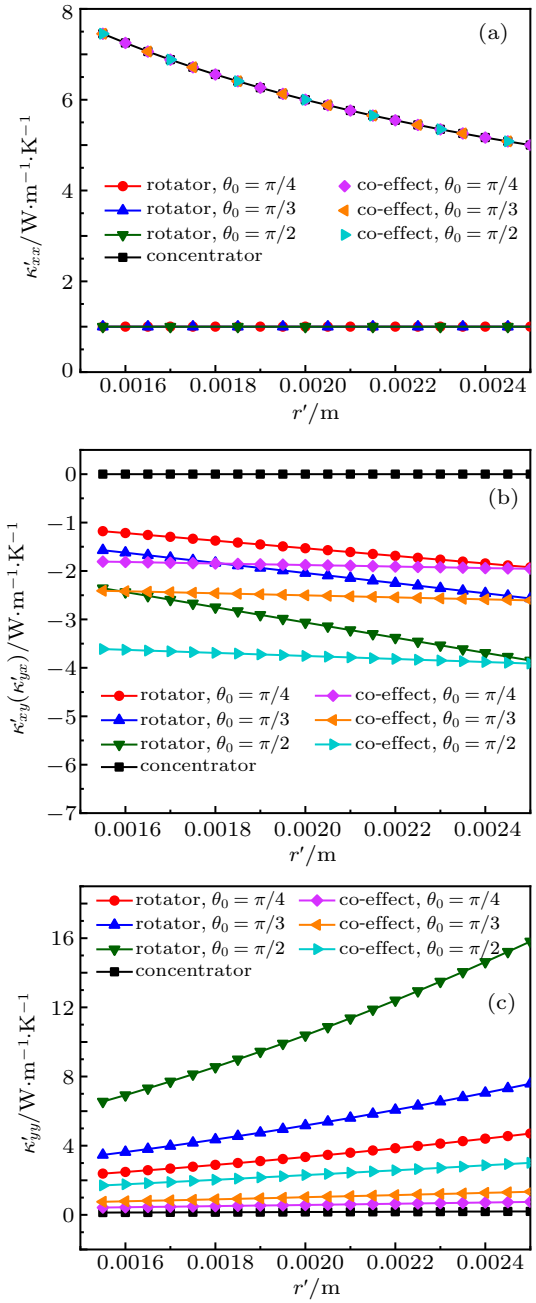

Fig. 5. Variations of different constitutes of anisotropic thermal conductivity in annuls from inner boundary to outer boundary of three structures: (a) κ'_{xx}, (b) κ'_{xy} (κ'_{yx}), (c) κ'_{yy}.

Only slight change occurs to the single concentrator since the curve is almost straight. Although all components essentially influence the heat propagation process, κ'_{yy} offers the largest contribution, the varying regulation corresponds to the thermal performance of the co-effect structure, which has additional rotation effect compared to the single rotator and owns more uniform energy distribution compared to the single rotator.

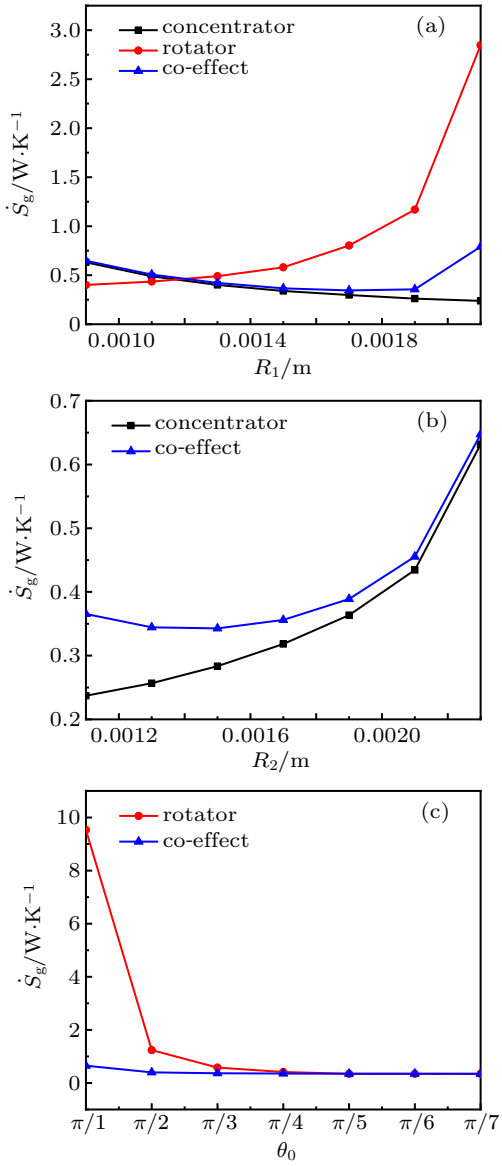

Fig. 6. Variations of the transformed total entropy generation $\dot{S}_g$ with different variables in three structures, the applied temperature gradient is 375 K/cm and $R_3 = 0.25$ cm: (a) $R_2 = 0.23$ cm, $\theta_0 = \pi/3$, (b) $R_1 = 0.09$ cm, $\theta_0 = \pi/3$, (c) $R_1 = 0.15$ cm, $R_2 = 0.23$ cm.

Taking engineering application value into account, the total entropy production is a more comprehensive and systematic index to investigate the irreversible energy loss and evaluate the quality of energy transfer processes. Applying the same temperature gradient along x axis and keeping R_3 as a constant, three geometric variables R_1, R_2, θ_0 are chosen and figure 6 shows the variations of the transformed total entropy generation $\dot{S}_g$ with different variables in three structures. It can be seen from Fig. 6(a) that $\dot{S}_g$ in the single concentrator exponentially decreases with the increase of R_1, indicat-

ing that smaller annuls region leads to less thermal energy loss of the single concentrator. $\dot{S}_g$ in the single rotator rapidly increases as R_1 increases, which is lower when $R_1 < 0.12$ cm but immensely higher than the value of the single concentrator thereafter, implying a more severe field perturbation. Variation of $\dot{S}_g$ in the co-effect structure is similar to the situation of single concentrator but the trend conversely changes when R_1 exceedes 0.17 cm. This change can be attributed to the rotation effect and the overall value of $\dot{S}_g$ in the co-effect structure is between the other two structures, which can be seen as a reflection of the compound action. In Fig. 6(b), $\dot{S}_g$ in the single concentrator increases monotonously with the increase of R_1. In the co-effect structure, $\dot{S}_g$ first drop a little, then increases with the same trend as the single concentrator and the lowest value appears at $R_2 = 0.15$ cm. With the increasing θ_0 in Fig. 6(c), $\dot{S}_g$ decreases first in both single rotator and the co-effect structure where the downtrend of the single rotator is more significant, then the changing gradient becomes smaller and two curves gradually approach straight lines, which almost overlap when θ_0 is smaller than $\pi/5$. Taken together, under fixed ambient conditions and R_3, the system consisting of the co-effect structure and outside environment possesses the minimum thermal energy loss and higher quality when $R_1 = 0.17$ cm and $R_2 = 0.15$ cm with smaller θ_0. The results are valuable for the further engineering applications of these flux-manipulating structures.

What is more, one thing needs to note about the co-effect structure proposed here, it can be a problem to fabricate the corresponding device due to the introduction of the off-diagonal components in the thermal conductivity tensors. By comparison, the single concentrator with only diagonal thermal conductivity components and the single rotator in traditional one are easier to realize.[15,20,21] It has been demonstrated that the transformation of heat conduction process can be generalized by using nonlinear materials with temperature-dependent thermal conductivities, materials whose shape vary with the change of ambient conditions (*i.e.*, shape memory alloys) are further used to implement intelligent thermal metamaterials.[32] Hence, considering existing devices with single function, it is possible to manufacture the co-effect device by combining the form as well as composition of the traditional concentrator with specific shape memory alloys. As ambient temperature changes, certain parts of alloys might deform, then possess the same shape as components in traditional rotator device. Through the cooperation of different parts of alloy with different functions, the co-effect device is potentially achieved, which can be explored as the in-depth expansion of the present work.

4. Conclusions

By applying coordinate distortions in different directions, a co-effect structure unifying concentration and rotation functions is proposed. From temperature profiles of the co-effect structure as well as the single concentrator and the single rotator, the structure with compound function not only enhanced the thermal energy density in the core region but also exhibited a more uniform thermal response with rotation effect. Considering the practical engineering value, distributions of the transformed local entropy production rate of three structures are compared. Results indicate that the concentration of heat flux can reduce the irreversible energy loss caused by rotation effect. The potential mechanism is explored by analyzing the characteristics of thermal conductivity constitutes in transformed domain. Finally, to better investigate the quality of the whole energy transfer process, variations of the transformed total energy production with chosen geometric parameters in different structures are studied and the system consisting of the co-effect structure and outside environment owns higher quality when $R_1 = 0.17$ cm and $R_2 = 0.15$ cm with smaller θ_0. The proposed co-effect structure can help to explore other potential mass/flux manipulating devices, the evaluation method from the view of thermodynamics has guiding significance for the further manufacturing and optimization of these devices in engineering applications.

References

[1] Pendry J B, Schurig D and Smith D R 2006 *Science* **312** 1780
[2] Schurig D, Mock J J, Justice B J, Cummer S A, Pendry J B, Starr A F and Smith D R 2006 *Science* **314** 977
[3] Ruan Z, Yan M, Neff C W and Qiu M 2007 *Phys. Rev. Lett.* **99** 113903
[4] Yan M, Ruan Z and Qiu M 2007 *Phys. Rev. Lett.* **99** 233901
[5] Chen H, Wu B I, Zhang B and Kong J A 2007 *Phys. Rev. Lett.* **99** 063903
[6] Alù A and Engheta N 2008 *Phys. Rev. Lett.* **100** 113901
[7] Andkjær J A and Sigmund O 2011 *Appl. Phys. Lett.* **98** 021112
[8] Andkjær J A, Mortensen N A and Sigmund O 2012 *Appl. Phys. Lett.* **100** 101106
[9] Chen H and Chan C T 2007 *Appl. Phys. Lett.* **91** 183518
[10] Li Q and Vipperman J S 2014 *Appl. Phys. Lett.* **105** 101906
[11] Cummer S A, Christensen J and Alù A 2016 *Nat. Rev. Mater.* **1** 16001
[12] Bückmann T, Thiel M, Kadic M, Schittny R and Wegener M 2014 *Nat. Commun.* **5** 1
[13] Kadic M, Bückmann T, Schittny R, Gumbsch P and Wegener M 2014 *Phys. Rev. Appl.* **2** 054007
[14] Guenneau S Amra C and Veynante D 2012 *Opt. Express* **20** 8207
[15] Fan C Z, Gao Y and Huang J P 2008 *Appl. Phys. Lett.* **92** 251907
[16] Chen T Y, Weng C N and Chen J S 2008 *Appl. Phys. Lett.* **93** 114103
[17] Schittny R, Kadic M, Guenneau S and Wegener M 2013 *Phys. Rev. Lett.* **110** 195901
[18] Xu H, Shi X, Gao F, Sun H and Zhang B 2014 *Phys. Rev. Lett.* **112** 054301
[19] Han T C, Bai X, Gao D L, Thong J T L, Li B W and Qiu C W 2014 *Phys. Rev. Lett.* **112** 054302
[20] Narayana S and Sato Y 2012 *Phys. Rev. Lett.* **108** 214303
[21] Han T C, Zhao J J, Yuan T, Lei D Y, Li B W and Qiu C W 2013 *Energy Environ. Sci.* **6** 3537
[22] Dai G L, Shang J and Huang J P 2018 *Phys. Rev. E* **97** 022129

[23] Hu R, Zhou S L, Li Y, Lei D Y, Luo X B and Qiu C W 2018 *Adv. Mater.* **30** 1707237
[24] Peng X Y and Hu R 2019 *ES Energy Environ.* **6** 39
[25] Hu R, Huang S Y, Wang M, Luo X B, Shiomi J and Qiu C W 2019 *Adv. Mater.* **31** 1807849
[26] Huang S Y, Zhang J W, Wang M, Hu R and Luo X B 2019 *ES Energy Environ.* **6** 51
[27] Zhou L L, Huang S Y, Wang M, Hu R and Luo X B 2019 *Phys. Lett. A* **383** 759
[28] Bejan A 1983 *Entropy generation through heat and fluid flow* (New York: John Wiley & Sons) pp. 475–475
[29] Torabi M and Aziz A 2012 *Int. Commun. Heat Mass Transfer* **39** 1487
[30] Xu G, Zhang H C, Zou Q, Jin Y and Xie M 2017 *Int. J. Heat Mass Transfer* **115** 682
[31] Xu G, Zhang H C, Zou Q and Jin Y 2017 *Int. J. Heat Mass Transfer* **109** 746
[32] Shen X Y, Li Y Jiang C R, Ni Y S and Huang J P 2016 *Appl. Phys. Lett.* **109** 031907